

# Synthesis, characterization, and redox behavior of six-coordinate (por)Ru(NO)Cl compounds (por = porphyrinato dianion)

Nan Xu <sup>a</sup>, Jonghyuk Lee <sup>a,\*</sup>, Douglas R. Powell <sup>b,1</sup>, George B. Richter-Addo <sup>a,\*</sup>

<sup>a</sup> Department of Chemistry and Biochemistry, University of Oklahoma, 620 Parrington Oval, Norman, OK 73019, USA

<sup>b</sup> X-ray Structural Laboratory, Department of Chemistry, University of Wisconsin, 1101 University Avenue, Madison, WI 53706, USA

Received 26 April 2004; accepted 26 June 2004

Available online 29 July 2004

Dedicated to the memory of the late Professor Rex E. Shepherd

## Abstract

A new high-yield preparative route to (por)Ru(NO)Cl compounds (por = porphyrinato dianion) from reactions of (por)Ru(NO)(alkoxide) precursors with boron trichloride is reported. These ruthenium nitrosyl chloride complexes are known to be useful precursors to (por)Ru(NO)-containing derivatives. The crystal structure of (OEP)Ru(NO)Cl (OEP = octaethylporphyrinato dianion) shows that the Ru–N–O linkage is linear. The redox behavior of the (por)Ru(NO)Cl compounds has been determined by cyclic voltammetry. Analysis of the data reveals that the first oxidation of the (por)Ru(NO)Cl compounds is porphyrin-ring centered.

© 2004 Elsevier B.V. All rights reserved.

**Keywords:** Porphyrin; Nitric oxide; Nitrosyl; Ruthenium; Halide; Alkoxide

## 1. Introduction

The signaling role of nitric oxide (NO) is intimately connected to its interaction with the iron porphyrin cofactor in the heme-containing guanylyl cyclase enzyme. NO is now known to interact with many other heme proteins and some of these interactions have physiological significance (reviewed in [1]). Ruthenium porphyrins have been used as models for iron porphyrins in cases where the iron nitrosyl derivatives were too unstable to isolate and characterize. For example, we reported the

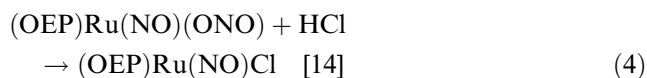
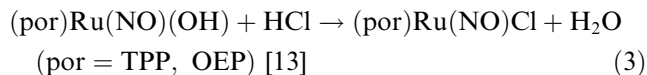
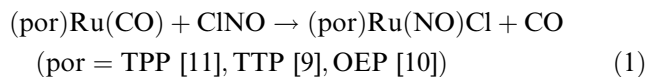
syntheses of stable six-coordinate nitrosyl thiolate compounds (OEP)Ru(NO)(SR) (SR = SCH<sub>2</sub>CF<sub>3</sub>, SC<sub>6</sub>F<sub>4</sub>H; OEP = octaethylporphyrinato dianion) [2] and also reported the X-ray crystal structure of (OEP)Ru(NO)(S-NACysMe) (NACysMe = *N*-acetyl-L-cysteinate methyl ester) [3] as a structural model of the NO adduct of ferric cytochrome P450, whose X-ray structure is not yet known. Other nitrosyl thiolate compounds of ruthenium porphyrins have been reported [4–8]. The organometallic compounds (por)Ru(NO)R (R = alkyl, aryl; por = porphyrinato dianion) [9,10] are also preparable from the chloride precursors by reaction with alkylating agents.

Importantly, useful starting reagents for the preparation of other ruthenium nitrosyl porphyrins are the (por)Ru(NO)Cl compounds. Their methods of preparation, to date, are shown in Eqs. (1)–(4) (TPP = tetraphenylporphyrinato dianion; TTP = tetratolylporphyrinato dianion).

\* Corresponding authors. Tel.: +1-4053256401; fax: +1-4053256111.

E-mail addresses: [jlee@chemdept.chem.ou.edu](mailto:jlee@chemdept.chem.ou.edu) (J. Lee), [griecher-addo@ou.edu](mailto:griecher-addo@ou.edu) (G.B. Richter-Addo).

<sup>1</sup> Present address: Crystallography Laboratory, Department of Chemistry, University of Kansas, Lawrence, KS 66045, USA.



We have previously shown that the nitrosyl alkoxides  $(\text{por})\text{Ru}(\text{NO})(\text{OR})$  can be prepared in high yields from the reaction of alkyl nitrites (RONO) with the precursor  $(\text{por})\text{Ru}(\text{CO})$  compounds via formal *trans* addition reactions [6,15]. We now show that the  $(\text{por})\text{Ru}(\text{NO})(\text{OR})$  compounds can be converted in quantitative yield (by IR and NMR spectroscopy) to the chloride derivatives  $(\text{por})\text{Ru}(\text{NO})\text{Cl}$  by reaction with boron trichloride. We have also investigated their redox properties by cyclic voltammetry.

## 2. Experimental

### 2.1. General

All reactions were performed under an atmosphere of prepurified nitrogen using standard Schlenk glassware and/or in an Innovative Technology Labmaster 100 Dry Box. Solutions for spectral studies were also prepared under a nitrogen atmosphere. Solvents were distilled from appropriate drying agents under nitrogen just prior to use:  $\text{CH}_2\text{Cl}_2$  ( $\text{CaH}_2$ ), hexane ( $\text{CaH}_2$ ).

### 2.2. Chemicals

The  $(\text{por})\text{Ru}(\text{NO})(\text{O}-i\text{-C}_5\text{H}_{11})$  ( $\text{por} = \text{TPP}$  [6],  $\text{TTP}$  [4],  $\text{OEP}$  [6]) compounds were prepared by the literature methods.  $(\text{T}(p\text{-OMe})\text{PP})\text{Ru}(\text{NO})(\text{O}-i\text{-C}_5\text{H}_{11})$  and  $(\text{T}(p\text{-CF}_3)\text{PP})\text{Ru}(\text{NO})(\text{O}-i\text{-C}_5\text{H}_{11})$  were also prepared as described for the TTP analogue.  $\text{BCl}_3$  (1.0 M in  $\text{CH}_2\text{Cl}_2$ ),  $\text{BBR}_3$  (1.0 M in  $\text{CH}_2\text{Cl}_2$ ), and  $\text{NBu}_4\text{PF}_6$  (98%) were purchased from Aldrich Chemical Co. and used as received. Chloroform-*d* (99.8%) was obtained from Cambridge Isotope Laboratories.

### 2.3. Instrumentation

Infrared spectra were recorded on a Bio-Rad FT-155 FTIR spectrometer. Proton NMR spectra were obtained on a Varian 300 MHz spectrometer and the signals referenced to the residual signal of the solvent

employed ( $\text{CHCl}_3$  at 7.26 ppm). All coupling constants are in hertz. FAB and ESI mass spectra were obtained on a VG-ZAB-E or a Micromass Q-TOF mass spectrometer, respectively. UV-Vis spectra were recorded on a Hewlett-Packard model 8453 diode array instrument. Wavelengths are reported with  $\epsilon$  values. Elemental analyses were performed by Atlantic Microlab, Norcross, GA.

Cyclic voltammetric measurements were performed using a BAS CV50W instrument (Bioanalytical Systems, West Lafayette, IN). A three-electrode cell was utilized and consisted of a 3.0-mm diameter Pt disk working electrode, a Pt wire counter electrode, and a  $\text{Ag}/\text{AgCl}$  reference electrode. Deaeration of all solutions was accomplished by passing a stream of high purity nitrogen through the solution for 10 min and then maintaining a blanket of nitrogen over the solution while performing the measurements. All experiments were performed on  $\text{CH}_2\text{Cl}_2$  solutions containing 0.1 M  $\text{NBu}_4\text{PF}_6$  at room temperature; under our conditions, 1.0 mM ferrocene displayed a redox couple at 0.37 V.

### 2.4. Synthesis

#### 2.4.1. $(\text{por})\text{Ru}(\text{NO})\text{Cl}$ ( $\text{por} = \text{TPP, TTP, T}(p\text{-OMe})\text{-PP, T}(p\text{-CF}_3)\text{PP, OEP}$ )

To a  $\text{CH}_2\text{Cl}_2$  solution (25 mL) of  $(\text{T}(p\text{-CF}_3)\text{PP})\text{Ru}(\text{NO})(\text{O}-i\text{-C}_5\text{H}_{11})$  (0.100 g, 0.091 mmol) was added  $\text{BCl}_3$  (0.12 mL, 1.0 M in  $\text{CH}_2\text{Cl}_2$ , 0.12 mmol). The color of the solution changed from red to dark red-purple over a 1 h period. The volume of the solution was reduced to ca. 5 mL and hexane (25 mL) was added to precipitate a dark red-purple solid. The supernatant solution was discarded and the solid was washed with hexane ( $3 \times 25$  mL) and dried in vacuo to give  $(\text{T}(p\text{-CF}_3)\text{PP})\text{Ru}(\text{NO})\text{Cl}$  (0.088 g, 0.084 mmol, 92% isolated yield). IR ( $\text{CH}_2\text{Cl}_2$ ,  $\text{cm}^{-1}$ ):  $\nu_{\text{NO}} = 1855$ .  $^1\text{H}$  NMR ( $\text{CDCl}_3$ ):  $\delta$  8.99 (s, 8H, pyrrole-H of  $\text{T}(p\text{-CF}_3)\text{PP}$ ), 8.42 (d, 8H,  $J = 8$  Hz, *o*-H of  $\text{T}(p\text{-CF}_3)\text{PP}$ ), 8.09 (m, 8H, *m*-H of  $\text{T}(p\text{-CF}_3)\text{PP}$ ). ESI mass spectrum:  $m/z$  1050 [ $(\text{T}(p\text{-CF}_3)\text{PP})\text{Ru}(\text{NO})\text{Cl} - \text{H}]^+$  (100%), 1016 [ $(\text{T}(p\text{-CF}_3)\text{PP})\text{Ru}(\text{NO})]^+$  (29%). UV-Vis spectrum ( $\lambda$  ( $\epsilon$ ,  $\text{mM}^{-1} \text{cm}^{-1}$ ),  $4.88 \times 10^{-6}$  M in  $\text{CH}_2\text{Cl}_2$ ): 331 (19), 412 (203), 465 (19 sh), 563 (12), 573 (10) nm.

The new  $(\text{T}(p\text{-OMe})\text{PP})\text{Ru}(\text{NO})\text{Cl}$  compound and the previously reported compounds  $(\text{por})\text{Ru}(\text{NO})\text{Cl}$  ( $\text{por} = \text{TPP}$  [11,13],  $\text{TTP}$  [5,9,12,16],  $\text{OEP}$  [13]) were also generated by this method in 82–90% isolated yields.

$(\text{T}(p\text{-OMe})\text{PP})\text{Ru}(\text{NO})\text{Cl}$ . IR ( $\text{CH}_2\text{Cl}_2$ ,  $\text{cm}^{-1}$ ):  $\nu_{\text{NO}} = 1851$ .  $^1\text{H}$  NMR ( $\text{CDCl}_3$ ):  $\delta$  9.06 (s, 8H, pyrrole-H of  $\text{T}(p\text{-OMe})\text{PP}$ ), 8.21 (m, 8H, *o*-H of  $\text{T}(p\text{-OMe})\text{PP}$ ), 7.33 (m, 8H, *m*-H of  $\text{T}(p\text{-OMe})\text{PP}$ ), 4.13 (s, 12H,  $\text{OCH}_3$  of  $\text{T}(p\text{-OMe})\text{PP}$ ). ESI mass spectrum:  $m/z$  864 [ $(\text{T}(p\text{-OMe})\text{PP})\text{Ru}(\text{NO})]^+$  (100%). UV-Vis spectrum ( $\lambda$  ( $\epsilon$ ,  $\text{mM}^{-1} \text{cm}^{-1}$ ),  $2.67 \times 10^{-6}$  M in  $\text{CH}_2\text{Cl}_2$ ): 319 (32), 417 (283), 571 (12) nm.

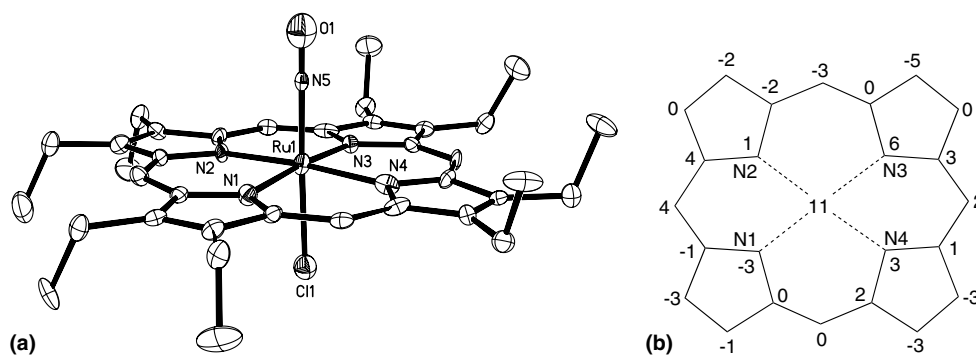


Fig. 1. (a) Molecular structure of (OEP)Ru(NO)Cl. Hydrogen atoms have been omitted for clarity. (b) Perpendicular atom displacements (in units of 0.01 Å) of the porphyrin core from the 24-atom mean porphyrin plane.

#### 2.4.2. (TTP)Ru(NO)Br

To a  $\text{CH}_2\text{Cl}_2$  solution (20 mL) of (TTP)Ru(NO)(O-*i*- $\text{C}_5\text{H}_{11}$ ) (0.050 g, 0.056 mmol) was added  $\text{BBR}_3$  (0.08 mL, 1.0 M in  $\text{CH}_2\text{Cl}_2$ , 0.08 mmol). The color of the solution changed from dark purple to dark green-purple over a 1 h period. The volume of the solution was reduced to ca. 5 mL and hexane (25 mL) was added to precipitate a dark green-purple solid. The supernatant solution was discarded and the solid was then washed with hexane (3×25 mL) and dried in vacuo to give (TTP)Ru(NO)Br·0.9 $\text{CH}_2\text{Cl}_2$  (0.040 g, 0.042 mmol, 74% isolated yield). *Anal.* Calc. for  $\text{C}_{48}\text{H}_{36}\text{N}_5\text{O}_1\text{Br}_1\text{Ru}_1 \cdot 0.9\text{CH}_2\text{Cl}_2$ : C, 61.42; H, 3.98; N, 7.32. Found: C, 61.53; H, 4.13; N, 7.04%. IR ( $\text{CH}_2\text{Cl}_2$ ,  $\text{cm}^{-1}$ ):  $\nu_{\text{NO}}=1847$ .  $^1\text{H}$  NMR ( $\text{CDCl}_3$ ):  $\delta$  9.04 (s, 8H, pyrrole-H of TTP), 8.16 (m, 8H, *o*-H of TTP), 7.59 (m, 8H, *m*-H of TTP), 5.28 (s,  $\text{CH}_2\text{Cl}_2$ ), 2.73 (s, 12H,  $\text{CH}_3$  of TTP). Low-resolution mass spectrum (FAB):  $m/z$  879 [(TTP)Ru(NO)Br] $^+$  (28%), 849 [(TTP)RuBr] $^+$  (20%), 800 [(TTP)Ru(NO)] $^+$  (100%), 770 [(TTP)Ru] $^+$  (94%). UV–Vis spectrum ( $\lambda$  ( $\epsilon$ ,  $\text{mM}^{-1}\text{cm}^{-1}$ ),  $4.08 \times 10^{-6}$  M in  $\text{CH}_2\text{Cl}_2$ ): 338 (21), 417 (247), 465 (21 sh), 486 (19), 578 (11) nm.

#### 2.5. X-ray crystallography

A suitable brown prism-shaped crystal of (OEP)Ru(NO)Cl· $\text{CH}_2\text{Cl}_2$  was adventitiously grown from the light-induced decomposition of (OEP)Ru(NO)(*t*Bu) in methylene chloride. Intensity data for this compound were collected using a Bruker SMART-CCD area detector mounted on a Bruker P4 goniometer using with graphite monochromated Mo  $\text{K}\alpha$  radiation ( $\lambda=0.71073$  Å). The intensity data, which nominally covered one and a half hemispheres of reciprocal space, were measured as a series of  $\phi$ -oscillation frames each of  $0.4^\circ$  for 45 s/frame. The detector was operated in  $512 \times 512$  mode and was positioned 5.00 cm from the sample. Coverage of unique data was 99.1% complete to  $25.00^\circ$  in  $\theta$ . Cell parameters were determined from a non-linear least squares fit of 4498 peaks in the range  $3.0^\circ < \theta < 25.0^\circ$ . The first 50 frames were repeated at

the end of data collection and yielded a total of 199 peaks showing a variation of 0.27% during the data collection. The data were corrected for absorption by the empirical method [17] giving minimum and maximum transmission factors of 0.727 and 0.831.

The monoclinic space group  $P2_1$  was determined by systematic absences and statistical tests and verified by subsequent refinement. The structure was solved by direct methods and refined by full-matrix least-squares methods on  $F^2$  [18]. Hydrogen atom positions were initially determined by geometry and refined by a riding model. Non-hydrogen atoms were refined with anisotropic displacement parameters. A total of 424 parameters were refined against 23 restraints and 7361 data to give  $wR(F^2)=0.1297$  and  $S=0.999$  for weights of  $w=1/[\sigma^2(F^2)+(0.0538P)^2]$ , where  $P=[F_o^2+2F_c^2]/3$ . The final

Table 1  
Crystal data and structure refinement

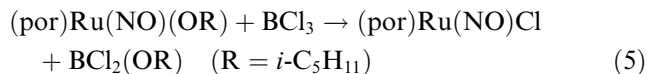
Formula	$\text{C}_{37}\text{H}_{46}\text{N}_5\text{OCl}_3\text{Ru}$
Formula weight	784.21
$T$ (K)	138(2)
Crystal system	monoclinic
Space group	$P2_1$
Unit cell dimensions	
$a$ (Å)	8.2156(8)
$b$ (Å)	20.796(2)
$c$ (Å)	10.8454(9)
$\alpha$ ( $^\circ$ )	90
$\beta$ ( $^\circ$ )	103.268(2)
$\gamma$ ( $^\circ$ )	90
$V$ (Å $^3$ ), $Z$	1803.5(3), 2
$D_{\text{calc}}$ ( $\text{g}/\text{cm}^3$ )	1.444
Absorption coefficient ( $\text{mm}^{-1}$ )	0.694
$F(000)$	812
Crystal size (mm)	$0.20 \times 0.14 \times 0.05$
$\theta$ range for data collection ( $^\circ$ )	1.96–28.30
Reflections collected	9125
Independent reflections	7361 [ $R_{\text{int}}=0.0383$ ]
Data/restraints/parameters	7361/23/424
Goodness-of-fit on $F^2$	0.999
$R$ ( $F$ observed data)	$R_1=0.0591$
$wR$ ( $F^2$ all data)	$wR_2=0.1297$
Largest difference of peak and hole ( $\text{e}/\text{Å}^3$ )	1.395 and $-1.190$

$R(F)$  was 0.0591 for the 5566 observed,  $[F > 4\sigma(F)]$ , data. The largest shift/s.u. was 0.000 in the final refinement cycle. The final difference map had maxima and minima of 1.395 and  $-1.190 \text{ e}/\text{\AA}^3$ , respectively. The absolute structure was determined by refinement of the Flack parameter [19]. The polar axis restraints were taken from Flack and Schwarzenbach [20]. Displacement ellipsoids in Fig. 1 are drawn at the 50% probability level. Details of the crystal data and refinement are given in Table 1 and Section 4.

### 3. Results and discussion

#### 3.1. Synthesis and characterization

Boron trichloride reacts with the (por)Ru(NO)(alkoxide) complexes to generate the (por)Ru(NO)Cl compounds in quantitative yields by IR and NMR spectroscopy of the crude product mixtures, and in high isolated yields. Thus, the reaction of (por)Ru(NO)(O-*i*-C<sub>5</sub>H<sub>11</sub>) (por = TPP, TTP, T(*p*-OMe)PP, T(*p*-CF<sub>3</sub>)PP, OEP) with the Lewis acid BCl<sub>3</sub> in CH<sub>2</sub>Cl<sub>2</sub> produces, after work-up, the (por)Ru(NO)Cl complexes in 82–92% isolated yields (Eq. (5)).



Two of these compounds (por = T(*p*-OMe)PP, T(*p*-CF<sub>3</sub>)PP) have not been reported previously. We also successfully extended this methodology to the new (TTP)Ru(NO)Br complex. Thus, (TTP)Ru(NO)Br was formed from the reaction of (TTP)Ru(NO)(O-*i*-C<sub>5</sub>H<sub>11</sub>) with BBr<sub>3</sub> in CH<sub>2</sub>Cl<sub>2</sub> in 74% isolated yield.

Ruthenium nitrosyl porphyrins display either linear or bent RuNO geometries. While most of the structurally characterized ruthenium nitrosyl porphyrins display linear RuNO groups [1], it is not always certain that the {RuNO}<sup>6</sup> porphyrin derivatives will display linear Ru–N–O bonds. For example, moderately bent RuNO bonds have been determined for (TTP)Ru(NO)(*p*-C<sub>6</sub>H<sub>4</sub>F) (152°) [9], (OEP)Ru(NO)(*p*-C<sub>6</sub>H<sub>4</sub>F) (155°) [10], (OEP)Ru(NO)(SCH<sub>2</sub>CF<sub>3</sub>) (161° and 157°) [1,21], and (TTP)Ru(NO)(NOsO<sub>3</sub>) (153°) [22]. We were thus interested in determining the structure of the axial group in (por)Ru(NO)Cl.

The molecular structure and the porphyrin atom displacements for (OEP)Ru(NO)Cl are shown in Figs. 1(a) and (b), respectively. To the best of our knowledge, this is the first reported crystal structure of a nitrosyl porphyrin chloride of any metal. Selected bond lengths and angles are listed in Table 2.

The Ru–N(O) and N–O bond lengths are 1.803(7) and 1.093(9) Å, respectively, and the RuNO group is essentially linear with a bond angle of 176.6(6)°. The axial

Table 2

Selected bond lengths and angles for (OEP)Ru(NO)Cl

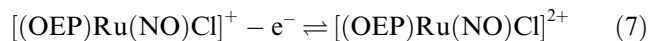
Bond lengths (Å)			
N(5)–O(1)	1.093(9)	Ru(1)–N(3)	2.048(5)
Ru(1)–N(5)	1.803(7)	Ru(1)–N(4)	2.055(7)
Ru(1)–N(1)	2.064(5)	Ru(1)–Cl(1)	2.331(2)
Ru(1)–N(2)	2.039(6)		
Bond angles (°)			
O(1)–N(5)–Ru(1)	176.6(6)	N(2)–Ru(1)–N(1)	90.0(2)
N(5)–Ru(1)–N(2)	92.8(2)	N(3)–Ru(1)–N(1)	174.8(2)
N(5)–Ru(1)–N(3)	93.2(2)	N(4)–Ru(1)–N(1)	89.8(2)
N(2)–Ru(1)–N(3)	89.6(2)	N(5)–Ru(1)–Cl(1)	178.2(2)
N(5)–Ru(1)–N(4)	92.4(3)	N(2)–Ru(1)–Cl(1)	88.6(2)
N(2)–Ru(1)–N(4)	174.9(3)	N(3)–Ru(1)–Cl(1)	85.73(16)
N(3)–Ru(1)–N(4)	90.2(2)	N(4)–Ru(1)–Cl(1)	86.26(18)
N(5)–Ru(1)–N(1)	92.1(2)	N(1)–Ru(1)–Cl(1)	89.04(17)

(O)N–Ru–Cl bond angle is 178.2(2)°. The Ru–N(por) bond lengths in (OEP)Ru(NO)Cl range from 2.039(6) to 2.064(5) Å, and the Ru atom is displaced by 0.11 Å from the 24-atom mean porphyrin plane toward the  $\pi$ -acid NO. The porphyrin moiety exhibits a slightly ruffled distortion. The axial Ru–Cl bond length of 2.331(2) Å is similar to the Ru–Cl length of 2.320(6) Å in [(OEP)RuCl]<sub>2</sub>( $\mu$ -O) [23], but is slightly shorter than the reported Ru–Cl length of 2.356(2) Å in (TTP)Ru(NS)Cl [16].

#### 3.2. Electrochemistry

The redox behavior of the (por)Ru(NO)Cl compounds (por = TPP, TTP, T(*p*-OMe)PP, T(*p*-CF<sub>3</sub>)PP, OEP) in CH<sub>2</sub>Cl<sub>2</sub> was examined at room temperature. The resulting cyclic voltammograms are shown in Fig. 2.

The (OEP)Ru(NO)Cl compound undergoes two reversible oxidations within the solvent potential limit (at  $E_{1/2} = +0.86$  and  $+1.38$  V versus Ag/AgCl). The separation in peak potentials,  $\Delta E_p = |E_{pa} - E_{pc}|$  is 78 mV for both the first and second oxidations, and this value is similar to that determined for the ferrocene–ferrocinium couple (80 mV) under identical conditions. We thus ascribed the first two oxidations to single-electron processes as shown in Eqs. (6) and (7).



In addition, these two oxidations are chemically reversible processes, with anodic to cathodic peak current ratios ( $i_{pa}/i_{pc}$ ) of  $\sim 1.0$ . Furthermore, plots of  $i_{pa}$  versus  $v^{1/2}$  for the first and second oxidations show linear relationships indicating that these processes are diffusion-controlled.

The (OEP)Ru(NO)Cl compound displays a quasi-reversible reduction peak at  $E_{pc} = -1.18$  V that is coupled to a weak return peak  $E_{pa}$  at  $-0.92$  V. This reduction

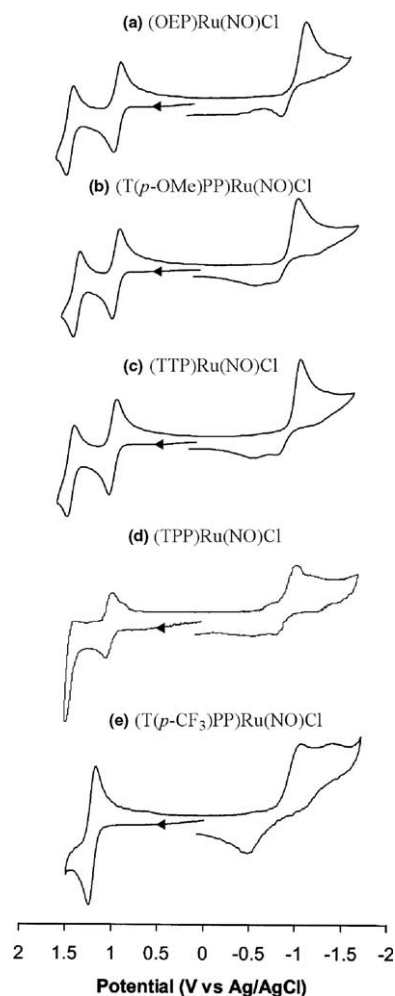


Fig. 2. Cyclic voltammograms of the (por)Ru(NO)Cl compounds (por=OEP (a), T(*p*-OMe)PP (b), TTP (c), TPP (d), and T(*p*-CF<sub>3</sub>)PP (e)) in CH<sub>2</sub>Cl<sub>2</sub> containing 0.1 M NBu<sub>4</sub>PF<sub>6</sub> and at a scan rate of 200 mV/s. The solubility of (TPP)Ru(NO)Cl in CH<sub>2</sub>Cl<sub>2</sub> is very low relative to the other compounds.

process is likely due to initial reduction followed by fast loss of chloride ion.

The cyclic voltammograms of the other compounds are also shown in Fig. 2. In general, all the (por)Ru(NO)Cl compounds undergo similar redox processes to that of the OEP derivative, however, the complexes con-

taining less electron-rich porphyrin macrocycles are harder to oxidize, and this is not unexpected. For example, the first oxidations of the (por)Ru(NO)Cl compounds occur at  $E_{1/2}$ =0.86 V (for OEP), 0.93 V (for T(*p*-OMe)PP), 0.97 V (for TTP), 1.04 V (for TPP), and 1.21 V (for T(*p*-CF<sub>3</sub>)PP), reflecting the decreasing electron-donor ability of the macrocycles. The electrochemical data are summarized in Table 3. The  $E_{1/2}$  for the first oxidation of (OEP)Ru(NO)Cl is lower than that of the four *para*-substituted TPP type compounds, consistent with the easier oxidation of the more electron-rich OEP macrocycle relative to the TPP type macrocycles. The increasing difficulty of oxidation with decreasing electron-donor ability of the porphyrin macrocycles makes the second oxidations of the TPP and T(*p*-CF<sub>3</sub>)PP derivatives inaccessible within the experimental solvent system range employed.

The examination of substituent effects on redox potentials in tetraaryl-substituted porphyrins provides very useful information regarding redox-active sites in metalloporphyrins. Thus, the correlation between half-wave potentials and the Hammett parameters ( $\sigma$ ) of the substituents can serve to infer the site of oxidation processes in metalloporphyrins [24]. In general, substituent effects on redox potentials are larger for porphyrin-ring centered redox reactions than for metal centered redox reactions in the case of substituted tetraarylporphyrins, and the average value of  $\rho$  for ring-centered redox processes has been determined to be  $70 \pm 10$  mV [24]. The plot of  $E_{1/2}$  versus Hammett parameter [25] (actually the sum of four times  $\sigma$  for the four phenyl groups) for the first oxidation of the four *para*-substituted tetraarylporphyrin compounds is shown in Fig. 3.

A linear relationship is obtained for the first oxidation of the compounds, with a calculated slope ( $\rho$ ) of 85 mV. Due to this relatively strong effect of substituents on redox potentials, we thus assign the first oxidations of the (por)Ru(NO)Cl compounds as porphyrin ring-centered oxidations. In related published work with several substituted tetraarylporphyrin (por)Co(NO) compounds, we showed that the related slope for the first oxidation of (por)Co(NO) was 76 mV which also corresponded to ring-centered oxidations [26]. Due to the limitations of accessible ranges in the solvent system

Table 3  
Half-wave and cathodic potentials for oxidations and reductions of (por)Ru(NO)Cl in CH<sub>2</sub>Cl<sub>2</sub>, 0.1 M NBu<sub>4</sub>PF<sub>6</sub>

Compound	$\sigma^a$	$E_{1/2}$		$E_{pc}$
		First oxidation	Second oxidation	Reduction
(OEP)Ru(NO)Cl		0.86	1.38	-1.18
(T( <i>p</i> -OMe)PP)Ru(NO)Cl	-0.27	0.93	1.35	-1.03
(TTP)Ru(NO)Cl	-0.17	0.97	1.43	-1.05
(TPP)Ru(NO)Cl	0.00	1.04		-1.00
(T( <i>p</i> -CF <sub>3</sub> )PP)Ru(NO)Cl	0.54	1.21		-1.05

<sup>a</sup> Hammett parameters taken from [25].

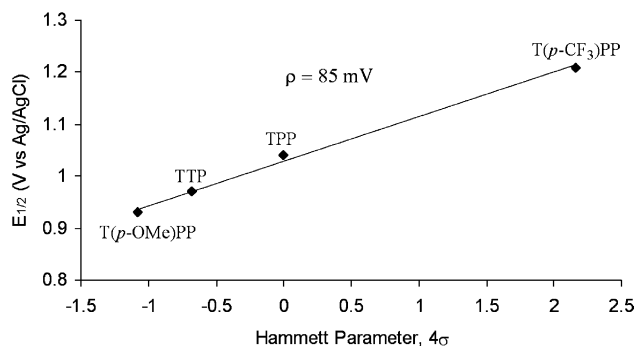


Fig. 3. Plot of  $E_{1/2}$  vs. the Hammett substituent constants for the first oxidation of (por)Ru(NO)Cl in  $\text{CH}_2\text{Cl}_2$ . Half-wave potentials are listed in Table 3.

employed, we are not able to assign the site of redox activity for the second oxidations (since the second oxidations of the TPP and T(p-CF<sub>3</sub>)PP complexes do not occur within the solvent potential limits).

To the best of our knowledge, there are only three other reports on the electrochemistry of ruthenium nitrosyl porphyrins [5,22,27]. The only previously published electrochemistry of a ruthenium porphyrin nitrosyl chloride was that of (TTP)Ru(NO)Cl [5], and our results are similar to those obtained from the previous study. Most (por)Ru(NO)-containing compounds display similar redox behavior to those reported here for the (por)Ru(NO)Cl compounds. Thus, they undergo one or two reversible oxidations, and generally irreversible or quasi-reversible reductions, except for (TPP)Ru(NO)(ONO) and [(TPP)Ru(NO)(H<sub>2</sub>O)]<sup>+</sup> [27]. In the latter study, a perchlorate salt was used as supporting electrolyte. Interestingly, the oxidation of [(TPP)Ru(NO)(H<sub>2</sub>O)]<sup>+</sup> was observed to be reversible to quasi-reversible, and (TPP)Ru(NO)(ONO) underwent replacement of the nitrito ligand by the perchlorate anion (from the supporting electrolyte) after oxidation.

#### 4. Supplementary material

CCDC 236941 contains the supplementary crystallographic data for this paper. These data can be obtained free of charge via [www.ccdc.cam.ac.uk/data\\_request/cif](http://www.ccdc.cam.ac.uk/data_request/cif), by emailing [data\\_request@ccdc.cam.ac.uk](mailto:data_request@ccdc.cam.ac.uk) or by contacting The Cambridge Crystallographic Data Centre, 12, Union Road, Cambridge CB2 1EZ, UK; fax: +44-1223-336033.

#### Acknowledgements

Support from the National Institutes of Health and the National Science Foundation (USA) is gratefully acknowledged. We thank Dr. Li Chen (USA) for experi-

mental assistance with obtaining suitable crystals of (OEP)Ru(NO)Cl.

#### References

- [1] L. Cheng, G.B. Richter-Addo, Binding and activation of nitric oxide by metalloporphyrins and heme, in: R. Guillard, K. Smith, K.M. Kadish (Eds.), *The Porphyrin Handbook*, vol. 4, Academic Press, San Diego, CA, 2000 (Chapter 33).
- [2] G.-B. Yi, M.A. Khan, G.B. Richter-Addo, *Inorg. Chem.* 35 (1996) 3453.
- [3] G.-B. Yi, M.A. Khan, G.B. Richter-Addo, *Chem. Commun.* (1996) 2045.
- [4] G.-B. Yi, L. Chen, M.A. Khan, G.B. Richter-Addo, *Inorg. Chem.* 36 (1997) 3876.
- [5] D.S. Bohle, C.-H. Hung, B.D. Smith, *Inorg. Chem.* 37 (1998) 5798.
- [6] J. Lee, G.-B. Yi, M.A. Khan, G.B. Richter-Addo, *Inorg. Chem.* 38 (1999) 4578.
- [7] J. Lee, G.-B. Yi, D.R. Powell, M.A. Khan, G.B. Richter-Addo, *Can. J. Chem.* 79 (2001) 830.
- [8] G.-B. Yi, M.A. Khan, D.R. Powell, G.B. Richter-Addo, *Inorg. Chem.* 37 (1998) 208.
- [9] S.J. Hodge, L.-S. Wang, M.A. Khan, V.G. Young Jr., G.B. Richter-Addo, *Chem. Commun.* (1996) 2283.
- [10] G.B. Richter-Addo, R.A. Wheeler, C.A. Hixon, L. Chen, M.A. Khan, M.K. Ellison, C.E. Schulz, W.R. Scheidt, *J. Am. Chem. Soc.* 123 (2001) 6314.
- [11] M. Massoudipour, K.K. Pandey, *Inorg. Chim. Acta* 160 (1989) 115.
- [12] D.S. Bohle, P.A. Goodson, B.D. Smith, *Polyhedron* 15 (1996) 3147.
- [13] I.M. Lorkovic, K.M. Miranda, B. Lee, S. Bernhard, J.R. Schoonover, P.C. Ford, *J. Am. Chem. Soc.* 120 (1998) 11674.
- [14] K.M. Miranda, X. Bu, I. Lorkovic, P.C. Ford, *Inorg. Chem.* 36 (1997) 4838.
- [15] G.B. Richter-Addo, *Acc. Chem. Res.* 32 (1999) 529 and references therein.
- [16] D.S. Bohle, C.-H. Hung, A.K. Powell, B.D. Smith, S. Wocadlo, *Inorg. Chem.* 36 (1997) 1992.
- [17] G.M. Sheldrick, *SADABS*. Program for Empirical Absorption Correction for Area Detector Data, University of Göttingen, Germany, 1996.
- [18] G.M. Sheldrick, *SHELXTL*: Structure Determination Software Suite, Madison, WI, USA, 1998.
- [19] H.D. Flack, *Acta Crystallogr., Sect. A* 39 (1983) 876.
- [20] H.D. Flack, D. Schwarzenbach, *Acta Crystallogr., Sect. A* 44 (1988) 499.
- [21] D.V. Fomitchev, P. Coppens, T. Li, K.A. Bagley, L. Chen, G.B. Richter-Addo, *Chem. Commun.* (1999) 2013.
- [22] W.-H. Leung, J.L.C. Chim, W. Lai, L. Lam, W.-T. Wong, W.H. Chan, C.-H. Yeung, *Inorg. Chim. Acta* 290 (1999) 28.
- [23] H. Masuda, T. Taga, K. Osaki, H. Sugimoto, M. Mori, H. Ogoshi, *Bull. Chem. Soc. Jpn.* 55 (1982) 3887.
- [24] K.M. Kadish, E. Van Caemelbecke, G. Royal, *Electrochemistry of metalloporphyrins in nonaqueous media*, in: K.M. Kadish, K.M. Smith, R. Guillard (Eds.), *The Porphyrin Handbook*, vol. 8, Academic Press, San Diego, CA, 2000, pp. 92–93 (Chapter 55).
- [25] C. Hansch, A. Leo, R.W. Taft, *Chem. Rev.* 91 (1991) 165.
- [26] G.B. Richter-Addo, S.J. Hodge, G.-B. Yi, M.A. Khan, T. Ma, E.V. Caemelbecke, N. Guo, K.M. Kadish, *Inorg. Chem.* 35 (1996) 6530 and (1997) 2696 [Erratum].
- [27] K.M. Kadish, V.A. Adamian, E.V. Caemelbecke, Z. Tan, P. Tagliatesta, P. Bianco, T. Boschi, G.-B. Yi, M.A. Khan, G.B. Richter-Addo, *Inorg. Chem.* 35 (1996) 1343.